

1 Formation of Reactive Nitrogen Oxides from Urban Grime

2 Photochemistry

3
4 **Alyson M. Baergen¹ and D. J. Donaldson^{1,2}**

5 ¹Department of Chemistry, University of Toronto, Toronto, M56 3H6, Canada

6 ²Department of Physical and Environmental Science, University of Toronto at Scarborough, Toronto, M1C
7 1A4, Canada

8
9 *Correspondence to:* D. J. Donaldson (jdonalds@chem.utoronto.ca)

10
11 **Abstract.** Impervious surfaces are ubiquitous in urban environments and constitute a substrate onto which
12 atmospheric constituents can deposit and undergo photochemical and oxidative processing, giving rise to
13 “urban grime” films. HNO₃ and N₂O₅ are important sinks for NO_x in the lower atmosphere and may be
14 deposited onto these films, forming nitrate through surface hydrolysis. Although such deposition has been
15 considered as a net loss of NO_x from the atmosphere, there is increasing evidence that surface-associated
16 nitrate undergoes further reaction. Here, we examine the gas phase products of the photochemistry of real,
17 field-collected urban grime using incoherent broadband cavity enhanced absorption spectroscopy
18 (IBBCEAS). Gas phase nitrogen oxides are emitted upon illumination of grime samples and their
19 production increases with ambient relative humidity (RH) up to 35% after which the production becomes
20 independent of RH. These results are discussed in the context of water uptake onto and evaporation from
21 grime films.

22 1. Introduction

23 Atmospheric NO_x (=NO+NO₂) is an important reactant in the formation of urban pollutants such as ground
24 level O₃, while HONO_(g) is an important photochemical source of OH (Finlayson-Pitts and Pitts, 1999).
25 Therefore, in order to quantify the local atmospheric oxidative capacity, it is important to understand the
26 processes mediating the concentrations of these species in the urban atmosphere. A major sink for nitrogen
27 oxides in the troposphere is the formation of gas phase HNO₃ or N₂O₅, followed by the deposition of these
28 species to surfaces and their subsequent hydrolysis to form nitrate. This anion is considered to be a sink for
29 the gas phase NO_x because its aqueous phase photochemistry is very slow. However, there is an increasing
30 body of literature which suggests that surface bound nitrate and HNO₃ are not terminal sinks, but rather can
31 undergo further recycling back to the gas phase. For example, HNO₃ has been shown to react on surfaces
32 with gas phase NO and HONO to form NO₂ (Mochida and Finlayson-Pitts, 2000; Rivera-Figueroa et al.,
33 2003; Saliba et al., 2001) and photochemical mechanisms for the conversion of HNO₃ and nitrate anion to
34 gaseous nitrogen oxide species have been proposed on a variety of surfaces including glass (Zhou et al.,

35 2003), snow (Grannas et al., 2007; Mochida and Finlayson-Pitts, 2000; Rivera-Figueroa et al., 2003; Saliba
36 et al., 2001), organic films (Handley et al., 2007), leaves (Zhou et al., 2011), plants (Ye et al., 2016),
37 building materials (Ye et al., 2016) and mineral oxide surfaces such as aluminum oxide and zeolite
38 (Gankanda and Grassian, 2013; Nanayakkara et al., 2014; Rubasinghege and Grassian, 2009; Schuttlefield
39 et al., 2008). There is particular interest surrounding whether such processes could explain an as of yet
40 unconfirmed source of daytime HONO in urban centers. Field studies have indicated that this missing
41 source is photochemical in nature and acts at or near ground level (Lee et al., 2015; Wong et al., 2013;
42 2012; Young et al., 2012). Other processes, such as reactions of NO_y (total reactive nitrogen) on aerosols
43 (Ma et al., 2013) and soil mediated processes (Oswald et al., 2013; Scharko et al., 2015), have also been
44 proposed but have not been confirmed at this time.

45 When studying atmospheric surface reactions, an often-overlooked surface is that of human-made
46 structures (eg. buildings, roadways). These surfaces, when exposed to the atmosphere, become coated in a
47 complex surface film over time due to the deposition and subsequent processing of atmospheric
48 constituents (Chabas et al., 2008; 2012; Diamond et al., 2000; Duigu et al., 2009; Favez et al., 2006;
49 Ionescu et al., 2006; Lam et al., 2005; Law and Diamond, 1998; Liu et al., 2003; Lombardo et al., 2010;
50 2005; Simpson et al., 2006; Wu et al., 2008a; 2008b). Referred to as “urban grime”, these films have
51 generally been thought of as merely a surface for deposition as a terminal sink for species. However, there
52 is increasing understanding that these films could also play a role in mediating environmental cycling.
53 Most attention has been brought to the idea that the films can sequester gas phase compounds and enhance
54 pollutant concentrations in rainfall runoff (Diamond et al., 2010; 2001; Priemer and Diamond, 2002), but
55 there is evidence suggesting that they can also impact the reactivity of species contained within the film,
56 such as PAHs (Ammar et al., 2010; Kwamena et al., 2007), and nitrate/HNO₃ (Baergen and Donaldson,
57 2013; Baergen et al., 2015).

58
59 Additionally, it has been predicted that there is enough water present on all environmental surfaces, even
60 those hydrophobic in nature, to influence heterogeneous reactions (Sumner et al., 2004). Rubasinghege and
61 Grassian have discussed the role of water on environmental surfaces outlining a wide range of mechanisms
62 through which water can impact reactivity (Rubasinghege and Grassian, 2013). These include altering
63 reaction pathways, promoting hydrolysis reactions, ionic dissociation and solvation of ions, inhibiting
64 reactivity through blocking reactive sites, enhancing ion mobility on the surface and altering the stability of
65 surface species. For example, both the extent of reaction and the distribution of products change as a
66 function of relative humidity (RH) for nitrate photolysis on aluminum oxide and Pyrex substrates but their
67 response is substrate dependant (Rubasinghege and Grassian, 2009; Zhou et al., 2003). Such studies have
68 generally investigated the impact of water on atmospheric surface chemistry by varying the ambient RH.
69 However, because different surfaces have different water affinities, they may be expected to display
70 different responses to changes in relative humidity. For example, a study by Nguyen *et al.* shows that
71 estimating water content in the aerosol, rather than just using RH data, is important for predicting the

72 formation of biogenic secondary organic aerosol (Nguyen et al., 2015). Related to grime surfaces, Sumner
73 *et al.* have shown how different surfaces, representing building surfaces, vary in their water uptake
74 behaviour (Sumner et al., 2004). There are only minimal studies performed looking at water interactions
75 with grime, but they show that grime films impact water uptake on surfaces (Baergen and Donaldson, 2013;
76 Chabas et al., 2014). Thus it is important to characterize the change in surface water content as a function
77 of RH as well as grime photochemistry. In the following we present results of experiments, which monitor
78 the photochemical release of gas phase nitrogen oxides from urban grime as a function of RH, in
79 conjunction with water uptake measurements on grime.

80

81 **2. Experimental**

82 **2.1 Sample collection**

83 Grime samples were collected by placing the substrate, either 3 mm diameter glass beads (Fisher Scientific)
84 or quartz crystal microbalance (QCM) crystals, outside in downtown Toronto, Canada for up to one year.
85 The beads were placed on metal mesh shelves underneath a building overhang, sheltering the sampler from
86 precipitation. Sunlight was blocked with a black cloth covering the front of the sample and a building
87 blocking the sunlight from the other direction. The QCM crystals were placed in holders where the face of
88 the crystal was facing the ground while the back was within the holder, preventing the collection of grime
89 on this backside, which would impact the QCM response. In this way both types of samples were shielded
90 from light and precipitation while still being open to the atmosphere.

91 **2.2 Incoherent Broad Band Cavity Enhanced Spectroscopy (IBBCEAS)**

92 Gas phase product formation was determined using IBBCEAS. The system is described in full elsewhere
93 (Reeser et al., 2013). Briefly, a 10 W LED with a maximum intensity at 372 nm, was focused into a 100 cm
94 cell. The cell was sealed with two highly reflective mirrors (>99.95% between 367nm and 380nm). The
95 light escaping through the back mirror was collected by a lens and focused onto a fiber optic bundle, which
96 was directed into a spectrograph with a CCD detector. The mirrors were continually purged using a flow
97 rate of 25 mL/min of N₂ directed onto the mirror surfaces. Transmission spectra were collected for 30 s
98 (averages of 30 scans with an integration time of 1 s each) over a wavelength range of 362 nm to 385 nm.

99 The concentrations of HONO and NO₂ were calculated using the method described by Fiedler and
100 Gherman (Fiedler et al., 2003; Gherman et al., 2008) and previously used by us (Reeser et al., 2013). This
101 uses measured mirror reflectivity (Washenfelder et al., 2008), Rayleigh cross sections of the carrier gas
102 (Bodhaine et al., 2010) and the absorption cross sections of NO₂ (Vandaele et al., 1998) and HONO (Stutz
103 et al., 2000) to fit the experimental spectra with DOASIS software (Lehmann, 2009). DOASIS uses a linear
104 least-squares method to fit the absorption bands to reference spectra and a polynomial to fit broad features
105 such as those from Rayleigh scattering, Mie scattering and temperature drifts. The fit is optimized by
106 including terms that allow for small shifts in absorption wavelengths and spread of peaks. A sample fit is

107 displayed as the solid line in Fig. 1. Calculated detection limits (signal/noise = 3) are 1.50×10^{11} molecules
108 cm^{-3} (~6ppb) for NO_2 and 6.5×10^{10} molecules cm^{-3} (~3ppb) for HONO.

109

110 **2.3 Photochemistry**

111 Samples of 10.0g of exposed glass beads were weighed into a glass petri dish for illumination. These were
112 placed within a stainless steel chamber (3.2" x 2.2" x 1.5") and nitrogen was flowed through the chamber
113 into the IBBCEAS cell at a rate of 0.3 L/min. RH and temperature in the chamber were monitored using a
114 Traceable® Memory Hygrometer/Thermometer. The reported accuracy is $\pm 2\%$ at mid-range and $\pm 4\%$
115 elsewhere in the range of 10 to 95% RH. The calibration was checked by measuring the RH above a series
116 of saturated salt solutions in comparison to the known deliquescent RH and was the same as the reported
117 values within the stated uncertainties.

118 Nitrogen was flowed through the system for one hour prior to illumination to establish a stable background
119 in the spectrum, and equilibrate the water vapour in the chamber for the RH used in the experiment. The
120 samples, initially at a RH of 35%, were illuminated through a quartz window at the top of the sample
121 chamber with a Xe arc lamp ($\lambda > 295\text{nm}$) for 60 min. The light was then blocked, the signal allowed to
122 return to baseline, and the RH adjusted for the next illumination period. After 60 min the sample was again
123 illuminated for 60 min before blocking the light and repeating the cycle for a third time. Average
124 concentrations were calculated for the second 30 min of illumination, where the signal appeared to reach
125 steady state, and then normalized to the initial steady state value at the RH of 35% to adjust for experiment
126 variability such as variations in sample, light intensity and temperature. These experiments were carried
127 out without temperature control, with the chamber operating at a temperature between 28 and 34 °C during
128 illumination.

129 Control experiments were carried out in which 10.0 g of clean beads were illuminated for one hour at a
130 relative humidity of 35%. In addition, 10.0 g of the grime coated beads were subjected to heating up to
131 36°C to study the impact of increased temperature on product formation. Both of these tests were
132 completed in triplicate with a different sample being used each time. Neither experiment showed
133 detectable levels of HONO or NO_2 .

134

135 The set up was further tested by flowing a known concentration of NO_2 through the empty chamber and
136 IBBCEAS cell. A flow containing 6.0 ppm NO_2 in N_2 was diluted in a stream of N_2 down to (4.76 ± 2.4)
137 $\times 10^{12}$ molecules/ cm^3 at varying RHs. NO_2 and HONO steady state concentrations measured at each RH
138 were used to characterize the IBBCEAS response to changes in humidity and the efficiency of NO_2
139 hydrolysis to HONO on the walls of the reaction chamber and IBBCEAS cell.

140

141 **2.4 Ion analysis**

142 Two different ion extraction techniques were used. For ion analysis of the illuminated beads, 4.0 g of
143 grime-coated beads were shaken for 5 minutes with 3.00 mL of deionized water with a resistivity of greater
144 than 18 MΩcm (Baergen et al., 2015). For ion analysis to accompany water uptake measurements, samples
145 were collected on 5 cm x 7.6 cm pieces of window glass over the same time period as the quartz crystals
146 and extracted with 45 mL deionized water. Glass samples were first placed in 25mL of water and sonicated
147 for 1 min. Each side of the glass was then washed twice with 5mL of water. Solutions were filtered
148 through a 0.2 μm IC Millex®-LG syringe filter before being analyzed by ion chromatography on a Dionex
149 ICS-2000. 1.33 mL samples were injected onto a concentrator/analytical column system: Ionpac® TAC-
150 ULP1/AS19 with KOH eluent for anion detection and Ionpac® TCC-ULP1/CS17 with methanesulfonic acid
151 eluent for cation detection. A second extraction resulted in concentrations of less than 10% of the first
152 extraction for all ions. The inorganic ion content of the grime used for photochemistry experiments is
153 given in Table S1.

154 2.5 Water Uptake

155 The mass of water taken up onto an urban grime film as a function of RH was measured using a quartz
156 crystal microbalance (QCM), as described in Demou et al (Demou et al., 2003). Grime was collected
157 directly onto a quartz crystal and then placed in the QCM. The QCM was housed in a plexiglass chamber
158 whose humidity was increased by flowing air through a water bubbler at room temperature at a variable
159 flow rate to maintain a rate of change of RH of 1%/min and decreased by flowing dry air through the
160 chamber at variable flow rates to maintain a rate of change of -1%/min. The frequency change of the
161 microbalance from the change in water content of the film was converted to a mass using the Sauerbrey
162 equation ($\Delta m = C\Delta f$) where Δm is the mass change, C is a proportionality constant and Δf is the frequency
163 change from the deposited mass. In a previous study, the Sauerbrey relationship was confirmed to hold for
164 this apparatus only up to 1% of the fundamental frequency of the crystal (Demou et al., 2003). Due to this
165 mass restriction, samples for QCM analysis were collected for only four weeks instead of the 1 year for the
166 photochemistry samples. The value of the constant C is reported to be $8.147 \times 10^7 \text{ Hz cm}^2 \text{ g}^{-1}$ for the 0.550
167 inch, 6 MHz crystals used in this study (Sauerbrey, 1959). The RH was measured using a Traceable®
168 Memory Hygrometer/Thermometer.

169 3 Results

170 3.1 Photochemical Production of nitrogen oxides

171 Figure 1 shows a typical absorption spectrum collected upon illumination of a grime sample. One can see
172 two features, typical of HONO absorption, a stronger signal at 368nm, and a second peak appearing at
173 384nm, at the longer edge of our wavelength range. The IBBCEAS is also sensitive to NO₂, which absorbs
174 in this wavelength region. However, this molecule was not detected in any of the photochemical
175 experiments performed here. We argue in the Supplementary Information that NO₂ hydrolysis on the walls
176 of the chamber and/or IBBCEAs cell via Eq. (1) (Finlayson-Pitts et al., 2002) would prevent NO₂ from

177 being detected even if it was originally formed in the chamber. Because of this hydrolysis there is an



178 uncertainty as to whether the HONO we observe in the illumination experiments was originally NO_2 , which
179 was hydrolyzed prior to detection, or if it is HONO being produced directly from the sample. Therefore,
180 we cannot attribute the observed HONO product exclusively to direct photochemistry of the grime sample;
181 rather we use the HONO signal to indicate the combined total emission of NO_2 and HONO. We further
182 note that the total product detected decreases when NO_2 is flowed through the apparatus in the light as
183 compared to in the dark by approximately 60%, indicating gas phase photolysis of products (see Fig. S1).
184 This highlights the importance of such considerations to be made whenever HONO and NO_2 are being
185 measured. Each system needs to be classified individually over a range of RH conditions.

186

187 Figure 2 depicts the results of a typical experiment where a grime sample is placed within the chamber and
188 exposed to three separate 60 min illumination periods at different relative humidities. The yellow
189 highlighted regions indicate illumination. It is clear that nitrogen oxides are released to the gas phase
190 during illumination and that the amount of products formed is dependent on the relative humidity. A repeat
191 illumination of a sample at an RH of 35% showed an average ratio of 0.88 ± 0.06 compared to the original
192 illumination. This provides evidence of some precursor depletion due to illumination, however, the much
193 smaller signals at 20% RH indicate that the RH dependence, apparent in Fig. 2, is related to the formation
194 of nitrogen oxides and not merely due to sample depletion. The nitrate to sulfate ratio of the grime before
195 and after illumination was used to examine nitrate behaviour. Sulfate is not expected to have any
196 photoreactivity on the film and thus was used to account for sample variability as was done in our previous
197 work (Baergen et al., 2015). No nitrate loss was detected between water extracts of beads before and after
198 illumination at 35% for three one-hour periods. The average change in the nitrate to sulfate ratio from
199 before to after illumination was 3.6 ± 6.6 %. There was also no nitrate loss detected for the samples that
200 were heated for three hours; these show an average change in the nitrate to sulfate ratio from before to after
201 heating of 1.0 ± 3.6 %. The amount of nitrate loss expected during illumination, based on the integrated
202 amount of gas phase nitrogen oxides produced, is in agreement with the above results.

203

204 In order to further investigate the RH dependence on product formation, the initial illumination period at
205 35% RH was used to normalize the concentrations detected for the next illumination periods. This data is
206 shown for a range of RH values in Fig. 3. Up to an RH of approximately 35% the amount of products
207 formed increases, after which product formation becomes independent of RH. At a RH of 0%, no products
208 were detected. However, from the NO_2 control experiments, there was evidence that gas phase
209 NO_2/HONO is lost to the chamber walls for these dry conditions, and thus this value was not reported.

210

211 **3.2 Water uptake by grime samples**

212 This interesting RH dependence of the amount of nitrogen oxides emitted photochemically from urban
213 grime motivates the study of water uptake onto grime. Grime-water interaction has been reported before
214 using ATR-FTIR with 1 week old grime, showing equilibrium with ambient water vapour (Baergen and
215 Donaldson, 2013). Chabas et al also reported that mass measurements on 100 month old films showed
216 enhanced water uptake on grime-coated substrates compared to clean ones (Chabas et al., 2014). Here we
217 use 4 week old samples collected throughout the year-long collection onto the glass beads, and look at both
218 water uptake and evaporation, to better probe water-grime interactions. The uptake and loss curves
219 displayed in Fig. 4 are an average of 16 curves collected at different time points through the year
220 normalized to the mass of major ions in the film (Cl^- , NO_3^- , SO_4^{2-} , Na^+ , K^+ , Mg^{2+} and Ca^{2+}), extracted from
221 a glass slide exposed to the atmosphere for the same length of time as the quartz crystal and scaled to the
222 same surface area as the crystal. The shaded region indicates the 95% confidence interval. The water uptake
223 onto a clean crystal was subtracted from each sample uptake before averaging, so the figure displays the
224 mass of water taken up mediated by the grime itself. The degree of uncertainty captures some of the
225 seasonality of grime water uptake, which will be discussed in an upcoming paper along with the seasonality
226 of grime ion content. The water uptake onto and evaporation from grime are both smooth curves, with no
227 indication of phase changes over the RH values spanned here. The lack of hysteresis also gives confidence
228 that the illumination experiments reflect the true state of the “real” urban grime, as the film remains
229 equilibrated with the ambient RH as this changes.

230

231 **4. Discussion**

232 The illumination of urban grime results in the release of gas phase nitrogen oxides in the form of NO_2
233 and/or HONO. While previously predicted (Baergen and Donaldson, 2013; Baergen et al., 2015), this is
234 one of the first observation of such gas phase products. Field-collected grime samples were illuminated,
235 without any alteration, clearly showing that urban grime is a source of nitrogen oxides back into the
236 atmosphere. Our previous work, as well as that of others, has shown that nitrate is present within urban
237 grime films (Favez et al., 2006; Lam et al., 2005) and that this nitrate is photolabile (Baergen and
238 Donaldson, 2013; Baergen et al., 2015; Ye et al., 2016). Nitrate photolysis is known to form NO_2 within
239 other media. Recent work by Ye *et al* also looked at surfaces exposed to the atmosphere for much shorter
240 exposure times detecting HONO and NO_2 at varying ratios depending on the surface (Ye et al., 2016). If
241 HONO is a product of this chemistry one possible source is via the protonation of nitrite, another known
242 product of aqueous nitrate photochemistry. However, our previous study was consistent with an alkaline
243 film due to the loss of ammonium, therefore we do not expect the film to be acidic enough for this
244 mechanism to be important (Baergen et al., 2015). The organic fraction of the film could also play a role in
245 the conversion of NO_2 to HONO, such as has been seen on organic surfaces such as humic acid (Stemmler
246 et al., 2006) and PAH films (Ammar et al., 2010). NO_2 to HONO conversion could also occur through NO_2
247 hydrolysis within the film. Although it seems likely that nitrate is responsible for the observed chemistry
248 due to its high concentration and known photoactivity on other surfaces, it is also possible that

249 photochemically active organo-nitrogen compounds may be present, though they have yet to be detected
250 within grime films. If present, these compounds may react as indicated by Han et al (Han et al., 2013) who
251 have reported the formation of R-NO, R-NO₂ and R-ONO₂ species on NO₂ exposed soot, which can
252 photolyze to form NO and HONO.

253

254 In contrast to our previous studies showing the photolability of nitrate in grime (Baergen and Donaldson,
255 2013; Baergen et al., 2015), the current study does not show nitrate depletion upon illumination. This
256 apparent discrepancy can be explained by the difference in experimental methods between studies. In both
257 previous studies, the films were “younger”, with between 1 and 6 weeks of collection time, in comparison
258 to the year-long collection here. In addition, for the Leipzig samples described in Baergen et al (Baergen et
259 al., 2015) the “light” sample was continually exposed to ambient sunlight, whereas in the present
260 experiment, like the previous Toronto study (Baergen and Donaldson, 2013), the samples were shielded
261 from the light for the entire collection and then illuminated in a controlled laboratory setting. Both of the
262 previous studies suggested that only a portion of the film is photolabile and the current result indicates that
263 this non-photoactive proportion of the film forms a greater proportion of the film over time. Continued
264 growth of the film may block photoactive sites or burry photoactive components of the film, making a
265 smaller portion available for reaction. Ye *et al* found a logarithmic relationship between surface density of
266 nitrate/HNO₃ and reaction rate (Ye et al., 2016) which could also indicate only nitrate/HNO₃ on the surface
267 remains reactive in comparison to the nitrate/HNO₃ within the film. Whether a film grown under continual
268 exposure to ambient light would show the same trend is an open question. Exposure to precipitation could
269 also impact the photoactive fraction, both in potential compositional changes as different fractions are
270 removed from the film during precipitation and in preventing such long-term film growth. This large non-
271 photoactive fraction may also explain the disparity between the depletion of gas phase products over time
272 and the lack of a corresponding nitrate drop; the photolabile fraction is small enough that the approximately
273 12% loss of reactive precursor implied by the gas phase result is too small of a proportion of the total
274 nitrate to be detected within the extracts of the whole film.

275

276 The photochemical release of gas phase NO₂ and/or HONO is clearly dependant on relative humidity and
277 therefore, as seen through the water uptake experiments, on the water content of the film. In particular, the
278 product formation increases as the amount of water on the film increases, up to a relative humidity of 35%
279 after which case, the chemistry is not impacted by further addition of water up to 60%. This behaviour is
280 different from what has been seen from nitrate photolysis experiments on other surfaces. In a study
281 performed on HNO₃ deposited on pyrex glass, the combined NO_x and HONO formation rate was highest at
282 0% and decreased for 20% and 50% while the reported HONO production rate was lowest at 0% and then
283 increased up to 80% (Zhou et al., 2003). However, the authors assumed a constant NO₂ to HONO wall
284 conversion independent of relative humidity taken from a measurement in a different system and thus the
285 determined ratios may not reflect the real distribution of products emitted as a result of the photochemistry

286 (Zhou et al., 2003). Humidity dependence has also been seen for nitrate photochemistry on mineral dust
287 surfaces. In this case, a minimum was seen for nitrate loss and NO₂ production at 0% and a maximum at
288 20% which subsequently decreased between 20 and 80%, while NO production continually decreased from
289 0 to 80% (Rubasinghege and Grassian, 2009). HONO production was not reported in this study.

290

291 The difference in nitrate photolysis behaviour between grime and other surfaces as a function of RH is
292 indicative of the grime providing a unique environment for the photochemistry. Many different
293 mechanisms for the role of water in surface reactions have been discussed, such as enhancing the mobility
294 of reagents, allowing them to move to more photolabile positions within in the film or enhanced hydrolysis
295 and dissociation of species such as HNO₃, NH₄NO₃ or N₂O₅ producing more of the photolabile precursors
296 (Rubasinghege and Grassian, 2013). The increased reactivity could also be the result of a viscosity change
297 within the film. It known that the viscosity of the particles changes based on relative humidity (Renbaum-
298 Wolff et al., 2013), and therefore, it is expected that the same would be true for the grime, with particles
299 being a source to the film. The film's water uptake/evaporation curve is consistent with continuous
300 viscosity change rather than phase transitions over the RH region studied. In a highly viscous film, the
301 photochemical products are more likely to be trapped and thus recombine. However, a less viscous film
302 would allow for faster diffusion and thus the release of products could become competitive and then
303 dominate in comparison to recombination. Such an impact has recently been suggested to explain a smaller
304 mass loss from illuminated SOA under low RH conditions in comparison to high (Wong et al., 2014), and
305 faster PAH ozonation within an SOA coated particles at high RH as compared to lower RH (Zhou et al.,
306 2013). This sort of behaviour would not be anticipated for a clean glass, or metal oxide surface. The
307 levelling off of product formation at relative humidities greater than 35% could indicate that a critical
308 amount of water has been reached. In the case of a viscosity effect, that would suggest that the process is
309 no longer diffusion limited. Another process that could be playing a role is the re-adsorption of the
310 products to the film, as discussed by Rubasinghege and Grassian (Rubasinghege and Grassian, 2009),
311 which would compete with further growth causing a net levelling off of product formation.

312

313 While specific atmospheric implications require a better speciation of products, the production of such
314 species can be discussed in the context of multiple recent field studies. In SHARP 2009, field
315 measurements that there was a photolytic source of HONO within 20m of the ground (Wong et al., 2012;
316 2013). Studies done in other urban centers such as London (Lee et al., 2015) and Los Angeles (Young et
317 al., 2012) also suggest there is an unknown photochemical HONO source. Many suggest that this source is
318 correlated to NO₂ however, in a study carried out in Bakersfield and Pasedena, the HONO source does not
319 correlate with NO₂ (Pusede et al., 2015). As discussed by those authors, the formation of HNO₃ and its
320 subsequent incorporation into aerosol as ammonium nitrate can extend the lifetime of airborne nitrate,
321 causing the nitrate which is deposited to not correlate temporally with NO_{2(g)}. Grime would likely have a
322 similar delayed response; in addition, the RH dependence of the grime photochemistry could serve as a

323 further mechanism for an offset in NO₂ values and HONO production, due to the cycling of RH conditions
324 in the atmosphere and therefore, the cycling of this source strength. However, more quantification and
325 speciation is required to evaluate the importance of such a grime source.

326

327 **5 Conclusions**

328 Urban grime was collected onto glass substrates without modification and illuminated. Grime
329 photochemistry produced nitrogen oxides in the form of NO₂ and/or HONO. Such chemistry is not
330 currently included in urban air models, but could impact NO_x and/or HONO levels in these centers. The
331 production of these species is dependant on RH, again highlighting the need to consider water content when
332 studying environmental surfaces.

333

334 **Acknowledgements**

335 This work was funded by NSERC. AMB thanks NSERC for a CGS-D award and the Government of
336 Ontario for an Ontario Graduate Scholarship.

337

338 **References**

- 339 Ammar, R., Monge, M. E., George, C. and D'Anna, B.: Photoenhanced NO₂ Loss on Simulated Urban
340 Grime, *Chem Phys Chem*, 11(18), 3956–3961, doi:10.1002/cphc.201000540, 2010.
- 341 Baergen, A. M. and Donaldson, D. J.: Photochemical renoxification of nitric acid on real urban grime,
342 *Environ Sci Technol*, 47(2), 815–820, doi:10.1021/es3037862, 2013.
- 343 Baergen, A. M., Styler, S. A., van Pinxteren, D., Muller, K., Herrmann, H. and Donaldson, D. J.: Chemistry
344 of Urban Grime: Inorganic Ion Composition of Grime vs Particles in Leipzig, Germany, *Environ Sci*
345 *Technol*, 49(49), 12688–12696, doi:10.1021/acs.est.5b03054, 2015.
- 346 Bodhaine, B. A., Wood, N. B., Dutton, E. G. and Slusser, J. R.: On Rayleigh Optical Depth Calculations, *J*
347 *Atmos Ocean Tech*, 16(11), 1854–1861, doi:10.1175/1520-0426(1999)016<1854:ORODC>2.0.CO;2,
348 2010.
- 349 Chabas, A., Alfaro, S., Lombardo, T., Verney-Carron, A., Da Silva, E., Triquet, S., Cachier, H. and Leroy,
350 E.: Long term exposure of self-cleaning and reference glass in an urban environment: A comparative
351 assessment, *Build Environ*, 79, 57–65, doi:10.1016/j.buildenv.2014.05.002, 2014.
- 352 Chabas, A., Lombardo, T., Cachier, H., Pertuisot, M. H., Oikonomou, K., Falcone, R., Verità, M. and
353 Geotti-Bianchini, F.: Behaviour of self-cleaning glass in urban atmosphere, *Build Environ*, 43(12), 2124–
354 2131, doi:10.1016/j.buildenv.2007.12.008, 2008.
- 355 Chabas, A., Lombardo, T., Verney-Carron, A. and Ausset, P.: Predicting the soiling of modern glass in
356 urban environments: A new physically-based model, *Atmos Environ*, 60(C), 348–357,
357 doi:10.1016/j.atmosenv.2012.06.050, 2012.
- 358 Demou, E., Visram, H., Donaldson, D. J. and Makar, P. A.: Uptake of water by organic films: the
359 dependence on the film oxidation state, *Atmos Environ*, 37(25), 3529–3537, doi:10.1016/S1352-
360 2310(03)00430-8, 2003.
- 361 Diamond, M. L., Gingrich, S. E., Fertuck, K., McCarry, B. E., Stern, G. A., Billeck, B., Grift, B., Brooker,

- 362 D. and Yager, T. D.: Evidence for Organic Film on an Impervious Urban Surface: Characterization and
363 Potential Teratogenic Effects, *Environ Sci Technol*, 34(14), 2900–2908, doi:10.1021/es9906406, 2000.
- 364 Diamond, M. L., Melymuk, L., Csiszar, S. A. and Robson, M.: Estimation of PCB Stocks, Emissions, and
365 Urban Fate: Will our Policies Reduce Concentrations and Exposure? *Environ Sci Technol*, 44(8), 2777–
366 2783, doi:10.1021/es9012036, 2010.
- 367 Diamond, M. L., Priemer, D. A. and Law, N. L.: Developing a multimedia model of chemical dynamics in
368 an urban area, *Chemosphere*, 44(7), 1655–1667, doi:10.1016/S0045-6535(00)00509-9, 2001.
- 369 Duigu, J. R., Ayoko, G. A. and Kokot, S.: The relationship between building characteristics and the
370 chemical composition of surface films found on glass windows in Brisbane, Australia, *Build Environ*,
371 44(11), doi:10.1016/j.buildenv.2009.02.019, 2009.
- 372 Favez, O., Cachier, H., Chabas, A., Ausset, P. and Lefevre, R.: Crossed optical and chemical evaluations of
373 modern glass soiling in various European urban environments, *Atmos Environ*, 40(37), 7192–7204,
374 doi:10.1016/j.atmosenv.2006.06.022, 2006.
- 375 Fiedler, S. E., Hese, A. and Ruth, A. A.: Incoherent broad-band cavity-enhanced absorption spectroscopy,
376 *Chem Phys Lett*, 371(3-4), 284–294, doi:10.1016/S0009-2614(03)00263-X, 2003.
- 377 Finlayson-Pitts, B. J. and Pitts, J. N., Jr: Chemistry of the upper and lower atmosphere: theory,
378 experiments, and applications, Academic Press, San Diego, California. 1999.
- 379 Finlayson-Pitts, B. J., Wingen, L. M., Sumner, A. L., Syomin, D. and Ramazan, K. A.: The heterogeneous
380 hydrolysis of NO₂ in laboratory systems and in outdoor and indoor atmospheres: An integrated mechanism,
381 *Phys Chem Chem Phys*, 5(2), 223–242, doi:10.1039/b208564j, 2002.
- 382 Gankanda, A. and Grassian, V. H.: Nitrate Photochemistry in NaY Zeolite: Product Formation and Product
383 Stability under Different Environmental Conditions, *J Phys Chem A*, 117(10), 2205–2212,
384 doi:10.1021/jp312247m, 2013.
- 385 Gherman, T., Venables, D. S., Vaughan, S., Orphal, J. and Ruth, A. A.: Incoherent Broadband Cavity-
386 Enhanced Absorption Spectroscopy in the near-Ultraviolet: Application to HONO and NO₂, *Environ Sci*
387 *Technol*, 42(3), 890–895, doi:10.1021/es0716913, 2008.
- 388 Grannas, A. M., Jones, A. E., Dibb, J., Ammann, M., Anastasio, C., Beine, H. J., Bergin, M., Bottenheim,
389 J., Boxe, C. S., Carver, G., Chen, G., Crawford, J. H., Dominé, F., Frey, M. M., Guzmán, M. I., Heard, D.
390 E., Helmig, D., Hoffmann, M. R., Honrath, R. E., Huey, L. G., Hutterli, M., Jacobi, H. W., Klán, P., Lefer,
391 B., McConnell, J., Plane, J., Sander, R., Savarino, J., Shepson, P. B., Simpson, W. R., Sodeau, J. R.,
392 Glasow, von, R., Weller, R., Wolff, E. W., Zhu, T. Zhu: An overview of snow photochemistry: evidence,
393 mechanisms and impacts, *Atmos Chem Phys*, 7, 4329–4373, doi:10.5194/acpd-7-4165-2007, 2007.
- 394 Han, C., Liu, Y. and He, H.: Heterogeneous photochemical aging of soot by NO₂ under simulated sunlight,
395 *Atmos Environ*, 64(C), 270–276, doi:10.1016/j.atmosenv.2012.10.008, 2013.
- 396 Handley, S. R., Clifford, D. and Donaldson, D. J.: Photochemical Loss of Nitric Acid on Organic Films: a
397 Possible Recycling Mechanism for NO_x, *Environ Sci Technol*, 41(11), 3898–3903, doi:10.1021/es062044z,
398 2007.
- 399 Ionescu, A., Lefèvre, R. A., Chabas, A., Lombardo, T., Ausset, P., Candau, Y. and Rosseman, L.: Modeling
400 of soiling based on silica-soda-lime glass exposure at six European sites, *Sci Total Environ*, 369(1-3), 246–
401 255, doi:10.1016/j.scitotenv.2006.04.009, 2006.
- 402 Kwamena, N.-O. A., Clarke, J. P., Kahan, T. F., Diamond, M. L. and Donaldson, D. J.: Assessing the

- 403 importance of heterogeneous reactions of polycyclic aromatic hydrocarbons in the urban atmosphere using
404 the Multimedia Urban Model, *Atmos Environ*, 41(1), 37–50, doi:10.1016/j.atmosenv.2006.08.016, 2007.
- 405 Lam, B., Diamond, M. L., Simpson, A. J., Makar, P. A., Truong, J. and Hernandez-Martinez, N. A.:
406 Chemical composition of surface films on glass windows and implications for atmospheric chemistry,
407 *Atmos Environ*, 39(35), 6578–6586, doi:10.1016/j.atmosenv.2005.07.057, 2005.
- 408 Law, N. L. and Diamond, M. L.: The role of organic films and the effect on hydrophobic organic
409 compounds in urban areas: an hypothesis, *Chemosphere*, 36(12), 2607–2620, doi:10.1016/S0045-
410 6535(97)10222-3, 1998.
- 411 Lee, J. D., Whalley, L. K., Heard, D. E., Stone, D., Dunmore, R. E., Hamilton, J. F., Young, D. E., Allan, J.
412 D., Laufs, S. and Kleffmann, J.: Detailed budget analysis of HONO in central London reveals a missing
413 daytime source, *Atmos Chem Phys Discuss*, 15, 22097–22139, doi:10.5194/acpd-15-22097-2015, 2015.
- 414 Lehmann, T.: DOASIS - DOAS Intelligent System, edited by Institute of Environmental Physics, [https](https://doasis.iup.uni-heidelberg.de)
415 doasis.iup.uni-heidelberg.de, 2009.
- 416 Liu, Q.-T., Chen, R., McCarry, B. E., Diamond, M. L. and Bahavar, B.: Characterization of Polar Organic
417 Compounds in the Organic Film on Indoor and Outdoor Glass Windows, *Environ Sci Technol*, 37(11),
418 2340–2349, doi:10.1021/es020848i, 2003.
- 419 Lombardo, T., Ionescu, A., Chabas, A., Lefèvre, R. A., Ausset, P. and Candau, Y.: Dose–response function
420 for the soiling of silica–soda–lime glass due to dry deposition, *Sci Total Environ*, 408(4), 976–984,
421 doi:10.1016/j.scitotenv.2009.10.040, 2010.
- 422 Lombardo, T., Ionescu, A., Lefèvre, R. A., Chabas, A., Ausset, P. and Cachier, H.: Soiling of silica-soda-
423 lime float glass in urban environment: measurements and modelling, *Atmos Environ*, 39(6), 989–997,
424 doi:10.1016/j.atmosenv.2004.10.030, 2005.
- 425 Ma, J., Liu, Y., Han, C., Ma, Q., Liu, C. and He, H.: Review of heterogeneous photochemical reactions of
426 NO_y on aerosol — A possible daytime source of nitrous acid (HONO) in the atmosphere, *J Environ Sci*,
427 25(2), 326–334, doi:10.1016/S1001-0742(12)60093-X, 2013.
- 428 Mochida, M. and Finlayson-Pitts, B. J.: FTIR Studies of the Reaction of Gaseous NO with HNO₃ on Porous
429 Glass: Implications for Conversion of HNO₃ to Photochemically Active NO_x in the Atmosphere, *J Phys*
430 *Chem A*, 104(43), 9705–9711, doi:10.1021/jp001471a, 2000.
- 431 Nanayakkara, C. E., Jayaweera, P. M., Rubasinghege, G., Baltusaitis, J. and Grassian, V. H.: Surface
432 Photochemistry of Adsorbed Nitrate: The Role of Adsorbed Water in the Formation of Reduced Nitrogen
433 Species on α -Fe₂O₃ Particle Surfaces, *J Phys Chem A*, 118(1), 158–166, doi:10.1021/jp409017m, 2014.
- 434 Nguyen, T. K. V., Capps, S. L. and Carlton, A. G.: Decreasing Aerosol Water Is Consistent with OC
435 Trends in the Southeast US, *Environ Sci Technol*, 49(13), 7843–7850, doi:10.1021/acs.est.5b00828, 2015.
- 436 Oswald, R., Behrendt, T., Ermel, M., Wu, D., Su, H., Cheng, Y., Breuninger, C., Moravek, A., Mouglin, E.,
437 Delon, C., Loubet, B., Pommerening-Roeser, A., Soergel, M., Poeschl, U., Hoffmann, T., Andreae, M. O.,
438 Meixner, F. X. and Trebs, I.: HONO Emissions from Soil Bacteria as a Major Source of Atmospheric
439 Reactive Nitrogen, *Science*, 341(6151), 1233–1235, doi:10.1126/science.1242266, 2013.
- 440 Priemer, D. A. and Diamond, M. L.: Application of the Multimedia Urban Model To Compare the Fate of
441 SOCs in an Urban and Forested Watershed, *Environ Sci Technol*, 36(5), 1004–1013,
442 doi:10.1021/es001397, 2002.
- 443 Pusede, S. E., VandenBoer, T. C., Murphy, J. G., Markovic, M. Z., Young, C. J., Veres, P. R., Roberts, J.

444 M., Washenfelder, R. A., Brown, S. S., Ren, X., Tsai, C., Stutz, J., Brune, W. H., Browne, E. C.,
445 Wooldridge, P. J., Graham, A. R., Weber, R., Goldstein, A. H., Dusanter, S., Griffith, S. M., Stevens, P. S.,
446 Lefer, B. L. and Cohen, R. C.: An Atmospheric Constraint on the NO₂ Dependence of Daytime Near-
447 Surface Nitrous Acid (HONO), *Environ Sci Technol*, 49(21), 12774–12781, doi:10.1021/acs.est.5b02511,
448 2015.

449 Reeser, D. I., Kwamena, N.-O. A. and Donaldson, D. J.: Effect of Organic Coatings on Gas-Phase Nitrogen
450 Dioxide Production from Aqueous Nitrate Photolysis, *J Phys Chem C*, 117, 22260–22267,
451 doi:10.1021/jp401545k, 2013.

452 Renbaum-Wolff, L., Grayson, J. W., Bateman, A. P., Kuwata, M., Sellier, M., Murray, B. J., Shilling, J. E.,
453 Martin, S. T. and Bertram, A. K.: Viscosity of α -pinene secondary organic material and implications for
454 particle growth and reactivity, *Proc Natl Acad Sci*, 110(20), 8014–8019, doi:10.1073/pnas.1219548110,
455 2013.

456 Rivera-Figueroa, A. M., Sumner, A. L. and Finlayson-Pitts, B. J.: Laboratory Studies of Potential
457 Mechanisms of Renoxification of Tropospheric Nitric Acid, *Environ Sci Technol*, 37(3), 548–554,
458 doi:10.1021/es020828g, 2003.

459 Rubasinghege, G. and Grassian, V. H.: Photochemistry of Adsorbed Nitrate on Aluminum Oxide Particle
460 Surfaces, *J Phys Chem A*, 113(27), 7818–7825, doi:10.1021/jp902252s, 2009.

461 Rubasinghege, G. and Grassian, V. H.: Role(s) of adsorbed water in the surface chemistry of environmental
462 interfaces, *Chem Commun*, 49(30), 3071–3094, doi:10.1039/c3cc38872g, 2013.

463 Saliba, N. A., Yang, H. and Finlayson-Pitts, B. J.: Reaction of Gaseous Nitric Oxide with Nitric Acid on
464 Silica Surfaces in the Presence of Water at Room Temperature, *J Phys Chem A*, 105(45), 10339–10346,
465 doi:10.1021/jp012330r, 2001.

466 Sauerbrey, G. Z.: Use of quartz vibration for weighing thin films on a microbalance, *J. Physik*. 1959.

467 Scharko, N. K., Schuette, U. M. E., Berke, A. E., Banina, L., Peel, H. R., Donaldson, M. A., Hemmerich,
468 C., White, J. R. and Raff, J. D.: Combined Flux Chamber and Genomics Approach Links Nitrous Acid
469 Emissions to Ammonia Oxidizing Bacteria and Archaea in Urban and Agricultural Soil, *Environ Sci
470 Technol*, 49(23), 13825–13834, doi:10.1021/acs.est.5b00838, 2015.

471 Schuttlefield, J., Rubasinghege, G., El-Maazawi, M., Bone, J. and Grassian, V. H.: Photochemistry of
472 Adsorbed Nitrate, *J. Am. Chem. Soc.*, 130(37), 12210–12211, doi:10.1021/ja802342m, 2008.

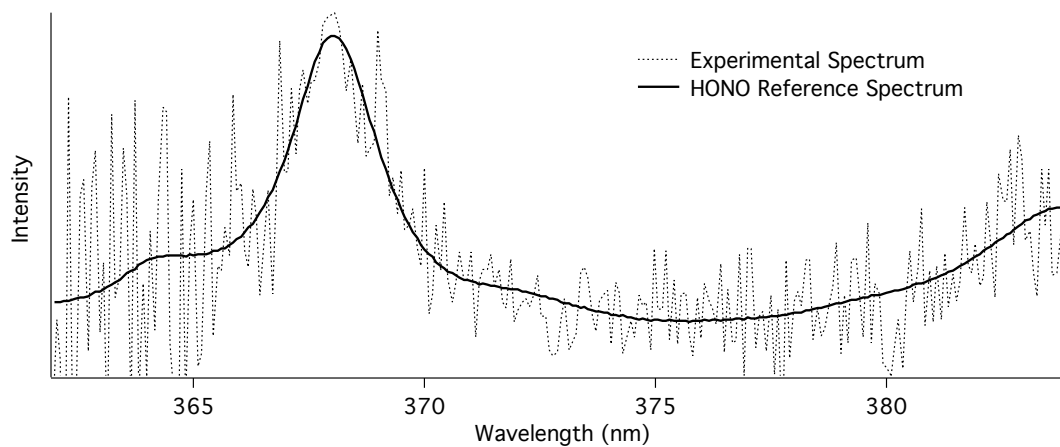
473 Simpson, A. J., Lam, B., Diamond, M. L., Donaldson, D. J., Lefebvre, B. A., Moser, A. Q., Williams, A. J.,
474 Larin, N. I. and Kvasha, M. P.: Assessing the organic composition of urban surface films using nuclear
475 magnetic resonance spectroscopy, *Chemosphere*, 63(1), 142–152, doi:10.1016/j.chemosphere.2005.07.013,
476 2006.

477 Stemmler, K., Ammann, M., Donders, C., Kleffmann, J. and George, C.: Photosensitized reduction of
478 nitrogen dioxide on humic acid as a source of nitrous acid, *Nature*, 440(7081), 195–198,
479 doi:10.1038/nature04603, 2006.

480 Stutz, J., Kim, E. S., Platt, U., Bruno, P., Perrino, C. and Febo, A.: UV-visible absorption cross sections of
481 nitrous acid, *J Geophys Res Atmos*, 105(D11), 14585–14592, doi:10.1029/2000JD900003, 2000.

482 Sumner, A. L., Menke, E. J., Dubowski, Y., Newberg, J. T., Penner, R. M., Hemminger, J. C., Wingen, L.
483 M., Brauers, T. and Finlayson-Pitts, B. J.: The nature of water on surfaces of laboratory systems and
484 implications for heterogeneous chemistry in the troposphere, *Phys Chem Chem Phys*, 6(3), 604–613,
485 doi:10.1039/b308125g, 2004.

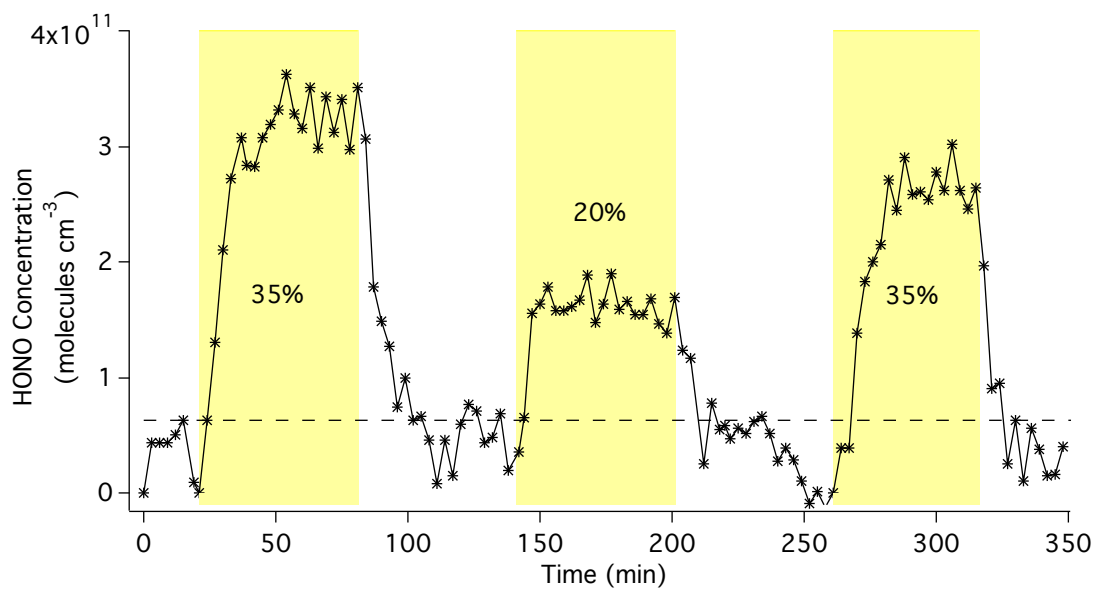
- 486 Vandaele, A. C., Hermans, C., Simon, P. C., Carleer, M., Colin, R., Fally, S., Mérienne, M. F., Jenouvrier,
487 A. and Coquart, B.: Measurements of the NO₂ absorption cross-section from 42 000 cm⁻¹ to 10 000 cm⁻¹
488 (238–1000 nm) at 220 K and 294 K, *J Quant Spectrosc Ra*, 59(3-5), 171–184, doi:10.1016/S0022-
489 4073(97)00168-4, 1998.
- 490 Washenfelder, R. A., Langford, A. O., Fuchs, H. and Brown, S. S.: Measurement of glyoxal using an
491 incoherent broadband cavity enhanced absorption spectrometer, *Atmos Chem Phys*, 8(24), 7779–7793,
492 doi:10.5194/acp-8-7779-2008, 2008.
- 493 Wong, J. P. S., Zhou, S. and Abbatt, J. P. D.: Changes in Secondary Organic Aerosol Composition and
494 Mass due to Photolysis: Relative Humidity Dependence, *J Phys Chem A*, doi:10.1021/jp506898c, 2014.
- 495 Wong, K. W., Tsai, C., Lefer, B., Grossberg, N. and Stutz, J.: Modeling of daytime HONO vertical
496 gradients during SHARP 2009, *Atmos Chem Phys*, 13(7), 3587–3601, doi:10.5194/acp-13-3587-2013,
497 2013.
- 498 Wong, K. W., Tsai, C., Lefer, B., Haman, C., Grossberg, N., Brune, W. H., Ren, X., Luke, W. and Stutz, J.:
499 Daytime HONO vertical gradients during SHARP 2009 in Houston, TX, *Atmos Chem Phys*, 12(2), 635–
500 652, doi:10.5194/acp-12-635-2012, 2012.
- 501 Wu, R. W., Harner, T. and Diamond, M. L.: Evolution rates and PCB content of surface films that develop
502 on impervious urban surfaces, *Atmos Environ*, 42(24), 6131–6143, doi:10.1016/j.atmosenv.2008.01.066,
503 2008a.
- 504 Wu, R. W., Harner, T., Diamond, M. L. and Wilford, B.: Partitioning characteristics of PCBs in urban
505 surface films, *Atmos Environ*, 42(22), 5696–5705, doi:10.1016/j.atmosenv.2008.03.009, 2008b.
- 506 [Ye, C., Gao, H., Zhang, N. and Zhou, X.: Photolysis of Nitric Acid and Nitrate on Natural and Artificial](#)
507 [Surfaces, *Environ Sci Technol*, doi:10.1021/acs.est.5b05032, 2016.](#)
- 508 Young, C. J., Washenfelder, R. A., Roberts, J. M., Mielke, L. H., Osthoff, H. D., Tsai, C., Pikelnaya, O.,
509 Stutz, J., Veres, P. R., Cochran, A. K., VandenBoer, T. C., Flynn, J., Grossberg, N., Haman, C. L., Lefer,
510 B., Stark, H., Graus, M., de Gouw, J., Gilman, J. B., Kuster, W. C. and Brown, S. S.: Vertically Resolved
511 Measurements of Nighttime Radical Reservoirs in Los Angeles and Their Contribution to the Urban
512 Radical Budget, *Environ Sci Technol*, 46(20), 10965–10973, doi:10.1021/es302206a, 2012.
- 513 Zhou, S., Shiraiwa, M., McWhinney, R. D., Poeschl, U. and Abbatt, J. P. D.: Kinetic limitations in gas-
514 particle reactions arising from slow diffusion in secondary organic aerosol, *Faraday Disc*, 165(0), 391–406,
515 doi:10.1039/c3fd00030c, 2013.
- 516 Zhou, X., Gao, H., He, Y., Huang, G., Bertman, S. B., Civerolo, K. and Schwab, J.: Nitric acid photolysis
517 on surfaces in low-NO_x environments: Significant atmospheric implications, *Geophys Res Lett*, 30(23),
518 2217, doi:10.1029/2003GL018620, 2003.
- 519 Zhou, X., Zhang, N., TerAvest, M., Tang, D., Hou, J., Bertman, S., Alaghmand, M., Shepson, P. B.,
520 Carroll, M. A., Griffith, S., Dusanter, S. and Stevens, P. S.: Nitric acid photolysis on forest canopy surface
521 as a source for tropospheric nitrous acid, *Nature Geoscience*, 4(7), 440–443, doi:10.1038/NCEO1164,
522 2011.
- 523



524

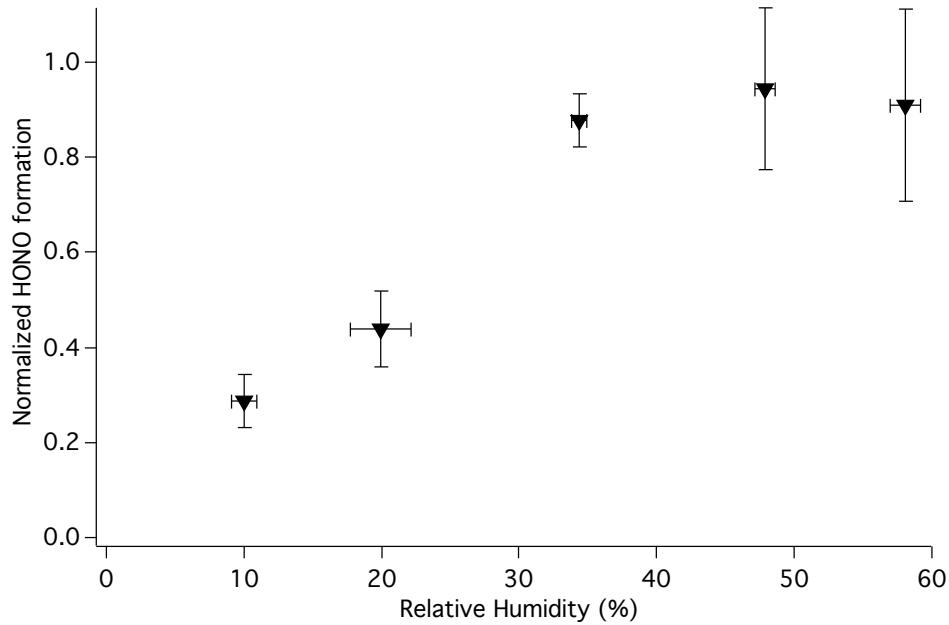
525 **Figure 1: Experimental absorption spectrum fit with a reference HONO spectrum (Stutz et al., 2000) using**
 526 **DOASIS (Lehmann, 2009). This spectrum was measured at RH = 37% and represents a concentration of**
 527 **2.17×10^{11} molecules cm^{-3}**

528



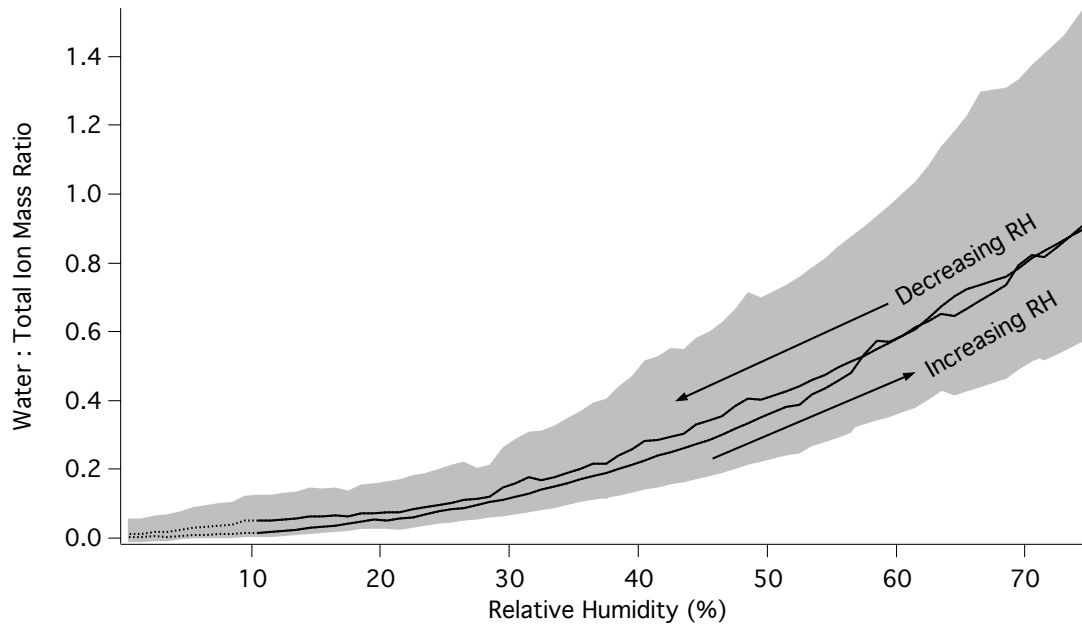
529

530 **Figure 2: Time trace of an experiment where the sections highlighted in yellow indicate when the sample is**
 531 **exposed to light. The relative humidity in the chamber during each illumination period is indicated. The HONO**
 532 **detection limit is indicated by the dashed line.**



533
534
535
536

Figure 3: HONO production as a function of relative humidity. Values are normalized to the steady state concentration of HONO formed during an initial illumination period at a relative humidity of 35%. The average of at least 3 measurements on different samples is shown; error bars represent 1 standard deviation.



537
538
539
540
541
542
543
544

Figure 4: Average ratio of water mass to total ion mass within grime as a function of relative humidity. Water uptake onto clean crystals was subtracted from the grime uptake curves and thus only grime-mediated uptake is shown here. The shaded region indicates a 95% confidence interval base on 16 measurements of different samples.

